Research on Engineering Structures & Materials
journal homepage: http://www.jresm.org
Research Group

Review Article

The evaluation of behavior of geopolymer reinforced concrete and conventional reinforced concrete beams: a critical review

Banu D. Handono[a], Ronny E. Pandaleke[b], Reynaldo J. Sela[c], Dody M.J. Sumajouw[*d], Steenie E. Wallah[e], Servie O. Dapas[f], Reky S. Windah[g]
Department of Civil Engineering, Sam Ratulangi University, Manado, Indonesia

Article Info

Article history:

Received 26 Mar 2023
Accepted 19 Jun 2023

Keywords:

Reinforced beams;
Conventional concrete;
Geopolymer;
Deflection;
Ductility

Abstract

As concrete technology has evolved, Geopolymer Concrete (GPC) has emerged as an ecologically friendly material compared to Ordinary Portland Cement (OPC) concrete, which has several complex environmental impacts. Without using OPC, which is typically used as a binder, the GPC has been developed. The base constituent material of GPC, like fly ash, is used to produce binder for geopolymer-reinforced concrete as an alternative. In building construction, the most frequently used component of the reinforced concrete element is a beam made by combining OPC concrete and steel reinforcement. This research involves a critical investigation of the bending behavior of control beams made of conventional reinforced concrete (CRC) and geopolymer reinforced concrete (GRC) beams. This critical review intentions to clarify how to differentiate a flexural behavior between GRC and CRC beams. Data from different experimental studies, which are divided into five parameters namely cracks and failure patterns, failure loads, load and deflection relationships, deflections, and ductility, provide the basis for the research. The results of the analytical review support the claim that the flexural behavior of the two beams exhibits similarities, and is quite typical. Therefore, it is possible to analyze and design GRC beams using the theory and standards used by CRC beams.

1. Introduction

Concrete remains a dominant material that cannot be separated from the construction industries. It is a versatile and proven construction material, capable of being utilized in various forms and finishes. When considering concrete for construction purposes, it is crucial to take into account its ease of use, durability, and simplicity of production However, past research indicates that the global man-made carbon dioxide (CO_2) released from the cement sector is approximately 8% of the overall. This is because producing OPC emits one ton of CO_2 into the atmosphere. Roughly 3.75 billion tons of OPC were manufactured worldwide in 2013 alone. It is projected that by 2050, an additional 4.4 billion tons of CO_2 will be released into the atmosphere due to the expected growth in cement consumption and production globally [1]. Therefore, there is a need to explore alternative binders for making concrete because the production of OPC contributes significantly to CO_2 emissions.

Initially, the mineral admixture is employed with positive outcomes as a partial replacement for cement. To create environmentally friendly concrete, a variety of industrial waste materials, including fly ash, are utilized to replace OPC [2]. The utilization of fly ash in GPC, a less conventional type of concrete, is a relatively recent advancement in concrete technology. Apart from fly ash, GPC is produced using waste materials for

[*]Corresponding author: dody_sumajouw@unsrat.ac.id
[a] orcid.org/0009-0003-3805-0388; [b] orcid.org/0009-0007-4232-642x; [c] orcid.org/0009-0005-2993-0177; [d] orcid.org/0000-0002-0135-6389; [e] orcid.org/0000-0001-5989-9581; [f] orcid.org/0009-0002-6482-8504; [g] orcid.org;/0009-0001-1532-8039
DOI: http://dx.doi.org/10.17515/resm2023.719st0326

example ceramic waste, clay, kaolin, blast furnace slag, palm oil clinker, rice husk ash, agricultural waste, and lime-based natural resources. For instance, Kaya, M [3] made GPC by combining powdered ceramic with Sodium Hydroxide (NaOH) and Sodium Silicate (Na2SiO3). Consequently, the application of industrial by-product materials in GPC is considered a viable environmentally friendly solution for future construction and building materials [4].

Davidovits [5] used the term "Geopolymer" to characterize a group of mineral binders based on silicoaluminates. In GPC, a single raw material or a mixture of various precursor materials can be utilized for polymerization [6]. Generally, alkaline activators are used to generate a geopolymer gel out of the silica and alumina that are already present in the source materials. Furthermore, the unreacted constituents and loose aggregates in the mixture are bonded together by the geopolymer gel that generates the GPC. Sodium or potassium silicate and sodium or potassium hydroxide have frequently been used as alkaline activators [7, 8, 9, 10, 11]. Additionally, sodium sulfate (Na_2SO_4) and sulfuric acid (H_2SO_4) were both present in the solution at 5% and 2% mass concentrations, respectively [12, 13, 14]. Polymeric Si-O-Al-O linkages in an amorphous form are generated by a chemical reaction on Si-Al minerals under highly alkaline circumstances. Additionally, the geopolymer material is said to have great fire resistance [15], and even in the presence of significant alkalinity, the alkali-aggregate interaction does not occur [5].

The novelty studies on making GPC are the utilization of low calcium Class F fly ash conducted by several experimental studies [16-23]. Additionally, the variables influencing the characteristics of geopolymers have been encountered by a number of research, as reported by Davidovits [24, 25, 26], for example geopolymer material achieves a compressive strength of 20 MPa, and between 70 and 100 MPa at the end of a 28-day curing period. Besides, fresh geopolymer is often cured at elevated temperatures because heat accelerates chemical processes. The mechanical strength is discovered to be significantly influenced by the curing time and form of activators [7, 9, 26]. Compressive strength increases dramatically while curing at 60^{o}C for 24 hours, resulting in a range of 47 to 53 MPa at one day [36]. Higher curing temperatures and longer curing times often provide materials with higher compressive strengths, but care must be made to prevent water loss during elevated temperatures curing. Though, using calcined raw materials of pure geological origin, such as metakaolin curing at ambient temperatures has been achieved successfully [5, 6, 8, 9, 10, 11, 25].

Even though fly ash-based geopolymers' mechanical strength is found to be significantly influenced by the curing time and variety of activators, the test findings from various investigations reveal that GPC cured at room temperature also produces results that are equivalent to those of heat curing [27-31]. GPC may reach its optimum 28-day strength at room temperature when slag or OPC material is added [32-36], and it can reach high strength at an earlier age when exposed to increased curing temperatures. The improved polymerization-induced intrinsic structure is what led to the improvement in physical characteristics [37, 38].

Despite having a higher tensile strength than OPC, GPC's behavior is still depending on the steel bars bonding and concrete. An important consideration for assessing the material's structural performance is the strength of bonding between the longitudinal reinforcement and the concrete. Because of its increased tensile strength, GPC exhibits a better bonding strength to the reinforcement [39–41]. The existing design formulas for bonding strength between reinforcement bars and CRC can still be applied to GPC since the failure behavior of GPC and CRC is similar [39-41]. Additionally, test results indicate that the GPC water content mixture, expressed as the water-to-geopolymer solid ratio, significantly affects its compressive strength [42]. Furthermore, fresh geopolymer concrete may be handled for

roughly 120 minutes without showing signs of setting and without reducing compressive strength [43]. Furthermore, the results of the experiments reveal that GPC has reduced creep [44]. Overall, fly ash-based GPC is very essential for building and construction, as a renewable cement substitute for green material [45]. This is because the usage of GPC may decrease the amount of CO_2 produced during the manufacture of OPC. The environmental harm carried on by the construction industry's CO_2 emissions could be minimized as a result of this.

Reinforced concrete beams play a vital role in supporting the loads in the building by withstanding them. The ability of the beam to resist failure under bending is referred to as flexural bending. To gain a deeper understanding of how beams behaves under bending, it is important to thoroughly comprehend five key parameters namely cracks and failure patterns, failure loads, load and deflection relationships, deflections, and ductility. These parameters are of utmost significance, and are commonly utilized by researchers to investigate the behavior of beams during bending. The reviewed study thoroughly examines and compares these parameters to enhance our understanding of how beams respond when is subjected to bending.

Previously, the investigation of reinforced GRC structural element behavior had received limited attention until a research team at Curtin University in Australia initiated a study on this topic [46-51]. Their research specifically focused on understanding the behavior of fly ash–based GRC structural members. Following this pioneering work, numerous studies on GRC structural members have been conducted and continue to be pursued.

Kumaravel et al. [52] examined the bending behavior of CRC control beams and GRC beams. The specimens were cast over an actual span of 3.200 mm, and they were put through monotonous load testing until failure. The beams were only supported, and they must withstand two concentrated loads that were distributed symmetrically across the beam span. Both types of beams' load with displacement responses were predicted through numerical analysis using the FEA software ANSYS. To compare with the theoretical findings, the displacement responses of the GRC and CRC beams were measured. The outcomes demonstrated greater flexural strength in the GRC beams. It was also found that the deflections at different stages were higher for GRC beams.

Furthermore, to evaluate the mechanical characteristics of GRC beams with CRC beams of equivalent grade, Abraham et al. [53] conducted experimental investigations. In this study, twenty beams, twelve GRC beam specimens, and eight CRC beam specimens were taken into consideration. All specimens were evaluated under two-point loads and were made with tensile reinforcement ratios of 0.55%, 0.83%, 1.02%, and 1.3%. Both kinds of beams' failure modes and the mechanical characteristics, such as load capacity, ultimate load, deflection, moment-curvature, first fracture load, crack width, and spacing, were examined. The test results show that when related to CRC beams of the same grade, GRC beams have better mechanical properties. This might be because the geopolymer paste bonds better than cement paste.

Dattatreya et.al [54] investigated the behavior of GRC beams. A total of 18 GRC beams, cured at room temperature, experienced flexure testing. The longitudinal reinforcement ratio was from 82 to 110 percent of the balanced condition, and the beam's dimensions were 100x150x1500 mm. All examples underwent two-point static loading testing. According to the report, the GRC beams' typical service loads were 12% lower than those of the CRC beams. The number, spacing, and width of the cracks, as well as the failure modes, were noted in the cracking patterns. With CRC beams, all produced essentially the same outcomes. The test results and the standard equations given by code to calculate the cracking and ultimate moment, and maximum deflection demonstrated a reasonable relationship even though they were not identical in all aspects.

Additionally, an experimental study on the short-term mechanical characteristics and flexural behavior of GRC and CRC beams was taken by Ojha, P.N., et al [55]. Geopolymer concrete with slag-fly ash based was used to make the GRC beams. It was discovered that GRC beams had short-term mechanical properties that were comparable to those of CRC beams in terms of flexural strength. Despite this, the modulus elasticity of the GRC beam was lower than the CRC beams for comparable strength. Moreover, this study demonstrated that both types of beams display comparable load-deflection relationships, yield loads, and yield moments. It was also determined, based on the noticeable cracks which were developed along the beam span, that the GRC beams and CRC beams exhibited a comparable quantity and type of cracks in flexure.

Also, in a study [56], fly ash was used in place of cement to a whole extent. By constructing a physical model in the form of reinforced concrete beams, laboratory testing was carried out. The structural beams with dimensions of 150x350 mm with a 4000 mm span were made to test the strength of GRC and CRC beams. ACI 437.1R-07 was followed while testing structural beams, and the outcomes of the laboratory tests were then contrasted with those of the theoretical analysis. Based on the test result, it was discovered that the strength of beams formed by GRC was practically identical to that of CRC. However, the findings of the theoretical analysis were lower than the structural capacity test results of both GRC and CRC beams.

Furthermore, Laskar et al. [57] found that GRC beams outperformed CRC beams in terms of capacity when subjected to cyclic loading effects. Compared to CRC beams, the GRC beams' capacity had increased by almost 30%. The GRC beams also demonstrated a slower rate of stiffness deterioration over time. The test findings also revealed that the GRC beams were about 45% more capable of dissipating energy than the CRC beams. This fact implies that the GRC beams can withstand earthquakes more effectively than the CRC beams.

The purpose and importance of this critical review are that it is essential to comprehend the distinction between pure bending and non-uniform bending of the GPC beams. In contrast to CRC beams, GRC beams have unique processes for the development of strength. Therefore, before using GRC beams in buildings for applications, the existing approaches for the analysis and design of GRC beams must be examined and confirmed with existing codes and standards applied for CRC beams.

2. Flexural Behavior of Conventional Reinforced Concrete (CRC) Beams

The loads acting on the beams result in deformational strain caused by the flexural stresses due to the externally applied load [58]. When the load is increased, a supplementary strain and deflection are continuously added to the beam, which causes additional deformation and strain resulting from flexural cracks along the span of the beam. Additional increases in the level of the load initiate failure of the beam. When the load reaches the beam's capacity, more cracks propagate along the beam. In such a situation eventually, the beam has no acceptable safety and reserve strength to support the applied load, and it can finally lead to the results of beam failure.

2.1. Failure Loads

The beam is expected to fail because it lacks the required safety and reserve strength to withstand the applied load. The failure modes of the CRC beam, as shown in Figure 1, can be grouped into three conditions namely the Balanced condition, Over-reinforced condition, and Under-reinforced condition [58]. These conditions are explained as follows:

- In the balanced condition, a beam section under flexure is considered to fail when the concrete strain exceeds the failure strain in bending compression, which is

typically equal to 0.003. At this point, the tensioned steel reaches its yield strain simultaneously that the concrete experiences failure strain.

- In the over-reinforced condition, the beam sections of reinforced concrete have an excess of reinforcement. In such cases, the failure occurs in the concrete before the steel reinforcement reaches its yield strain. If these beams are constructed and loaded to their maximum capacity, the tensioned steel will not yield significantly until the concrete achieves its maximum strain of 0.003.
- In the under-reinforced condition, the beam section refers to the situation where steel reinforcement in a reinforced concrete section fails by yield before the occurrence of concrete failure. The yielding of steel reinforcement indicates failure, and it occurs at loads smaller compared to those at which the concrete approaches its failure strain.

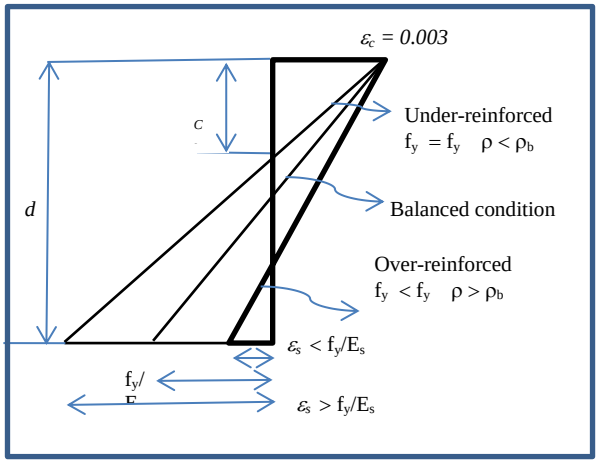

Fig. 1 Cross-section strain distribution [58]

2.2. Load and Deflection Relationship

A load-deflection relationship of CRC beams can be essentially idealized into a trilinear shape. The best possible load-deflection curve for mid-span beams is depicted in Figure 2. These occurrences are identified in the sequence as follows: initial cracking at point A, tensile reinforcing yielding at point B, crushing of concrete in the compression zone accompanied spalling of concrete cover at point C, and failure of the concrete compression zone due to reinforcement steel buckling at point D. Such sequential points are typical CRC beam flexural characteristics [59].

Three regions for the distinctive relationship of load-deflection for CRC beam are explained in three regions that are Pre-crack level (region I), Post-crack load level (region II), and Post serviceability crack level (region III) [59].

2.3. Crack and Failure Pattern

The type of failure that occurs in the beam structural elements depends on the cross-sectional stiffness (EI) of the beams. Flexural failure, shear compression failure, and diagonal tension failure are the three types of failure [58]. The type of failure for all literature on this study is considered a flexural failure.

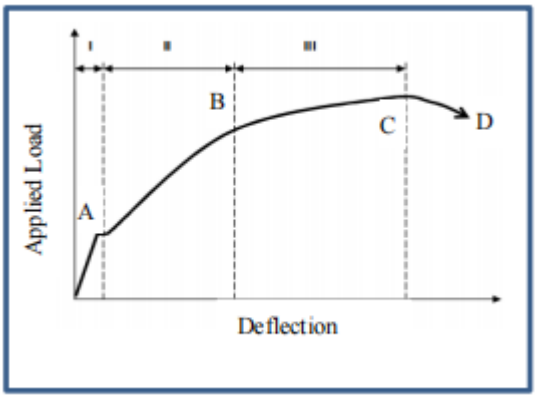

Fig. 2 Relationship between Load-Deflection for CRC Beam [59]

2.4. Deflection

The most essential aspect of reinforced concrete beams is the deflection problem. If the beam has a long span, the value of the deflection will also be large, and to reduce the deflection is usually by increasing the cross-sectional stiffness (EI). Mechanically the relationship of deflection (υ), cross-sectional strength (EI), and bending moment (M) is:

$$\frac{d^2v}{dx^2} = \frac{M}{EI} \tag{1}$$

Using the differential equation, the deflection for a beam supported by simple supports with the load (P) at the middle of the beam mid-span is:

$$\delta = v_{max} = \frac{PL^3}{48\ x\ EI} \tag{2}$$

The maximum amount of deflection that occurs as a result of uniform load (q) and concentrated load (P) can be specified by using equation (3).

$$\delta = \frac{5}{384} q \frac{L^4}{EI} + \frac{Pa}{48EI}(3L^2 - 4a^2) \tag{3}$$

2.5. Ductility

Ductility behavior due to loading on the beam with a load exceeding the ultimate load can be illustrated in Figure 3 [59]. The difference between brittle and ductile behavior can be seen in contrast.

The ratio of maximum to yield deflection, stated by the following equation, can be used to quantitatively estimate the ductility of a beam:

$$\mu_d = \frac{\Delta_u}{\Delta_y} \tag{4}$$

where:

μ_d = ductility of beam
Δ_u = maximum deflection
Δ_y = yield deflection

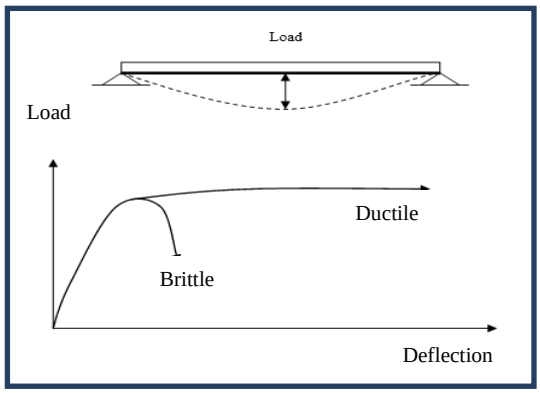

Fig. 3. Deflection Behavior Due to Loading

3. Methodology

In this study, the critical review is conducted based on data from various experimental studies which are grouped into five parameters, namely cracks and failure patterns, failure loads, load and deflection relationships, deflections, and ductility from both types of beams. The most significant indicator for comprehending the bending behavior of beams is understanding those five parameters. The study's progress is displayed as follows:

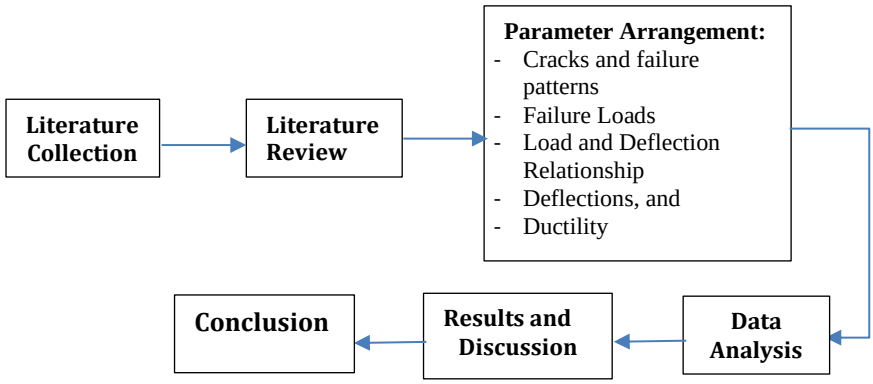

3.1. Materials and Mix Proportion

The experimental study presented in Research Report GC-1 by Hardjito and Rangan [32] was commonly prepared by most researcher to develop the mixture proportions of low-calcium fly ash-based GPC. Three composition mixtures were chosen for generating 40, 50, and 75 MPa compressive strengths [47]. Table 1 contains detailed mix combinations of GPC.

Dattatreya et.al [54], studied GRC beams that were made using various binder configurations, curing at room temperature, and having compressive strengths varying from 17 to 63 MPa. As the control (CRC) beams of the test examples, OPC, drinking water, fine aggregates, and coarse aggregates that complied with IS 12269 were used. Conventional concrete mixes prepared for CRC beams suggested by standards of IS 10262:2009 and ACI 211.1 were made to compare the outcomes of tests carried out using GRC beams.

In this study [56], physical models of the beams were made in 2 (two) variations of the mixture. The first mixture is GRC beams with 100% fly ash, and the second mixture is conventional reinforced concrete (CRC) beams with the use of 100% OPC.

Ojha et. al [55] investigated the mix design detail for the GRC beam dan CRC beam for normal and high-strength concrete. The CRC beam was designed according to IS 10262: 2009. The ratio of aggregate had been maintained at 60%: 40% of coarse aggregate to fine aggregate for normal-strength concrete mix [M40], and 35%: 65% for high-strength concrete mix [M70]. All the concrete mixes were kept between 75-100 mm for slump value. Superplasticizer was used for CRC beam mixes to reach the required slump value.

Table 1. The Detail Mix Composition of GPC [47]

Material	Mass (kg/m^3)
Aggregates (10mm)	550
Aggregates (7mm)	550
Fine Sand	640
Fly ash	404
Sodium hydroxide solution (14M)	41
Sodium silicate solution	102
Superplasticizer	6.0
Extra water*	GBI=25.5; GBII=17.0; GBIII= 13.5

* The amount of additional water added is the only difference between the three mixes.

3.2. Specimen Details and Test Set Up

To determine the cross-sectional capacity of GRC beams and CRC beams, physical models of the beam examples were created to carry out loads as shown in Figure 4 [56]. The compressive strength and tensile splitting test of both types of concrete were evaluated using the cylinder and beam specimens.

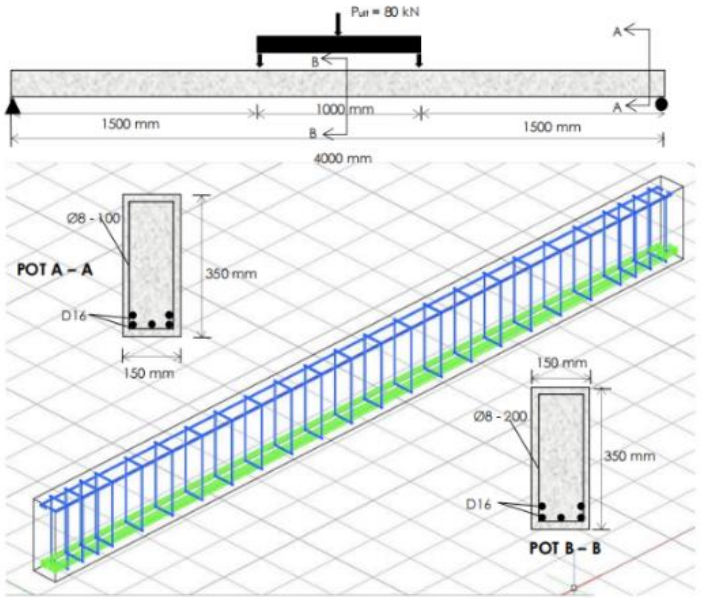

Fig. 4 Longitudinal reinforcement of GRC beam and CRC beam [56]

To prevent cracks due to sliding near the supports, and to ensure that a crack happens in the mid of the span (on the maximum moment), reinforced concrete cross sections were constructed with a specific amount of tensile reinforcement. The test configuration is displayed in Figure 5 below [56].

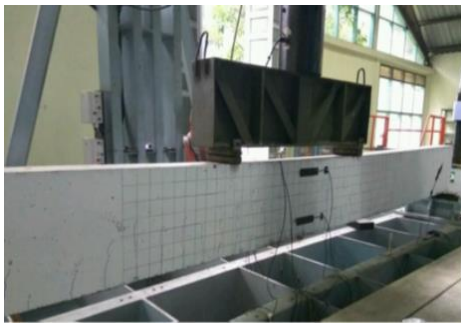

Fig. 5 Test Configuration for CRC beam Flexural Test [56]

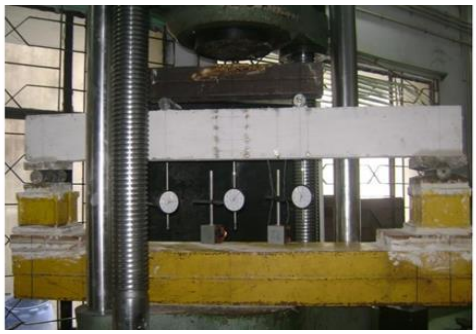

Fig. 6 Test Arrangement for Flexure [54]

Figure 6 depicts the configuration for the flexural test [54]. The 1000kN capacity Universal Machine Test (UTM) was used to test the beam specimen. To quantify deflections at the midspan and under the load locations, dial gauges were used. At various load levels, the dial gauge readings were verified. The load was set at 2.5kN intervals until the first crack was noticed. Following that, the load was increased in 5kN increments.

The simply supported beam over a 3000mm span, was put under two concentrated loads that were distributed symmetrically across the span [52]. Several Linear Variable Data Transformers (LVDTs) were positioned under the beam's load spots and in the middle of the span. The load was delivered in 2.5kN intervals. Figure 7 depicts the test configuration.

The 500kN capacity of the Flexural Testing Machine was used to test the beam prototype [55]. Every beam was intended to fail simply from pure bending. The beam was merely about 2400 mm long span, and 2000 mm clear beam span, and was put to two concentrated static point loads that were applied symmetrically to the span. The examples were cured at 27 ± 2oC ambient temperature and at least 65% relative humidity. Figure 8 depicts the load-test configuration for a beam in flexure.

Fig. 7 Test Configuration for Flexure [52]

Fig. 8 Test Configuration for Beams [55]

4. Findings and Discussion

4.1. Cracks pattern and failure mode

The cracking pattern on the beams can be observed in Figures 9. a [56] for the CRC beam and 9. b [47] for the GRC beam. The specimen's failure pattern was confirmed, and both beams exhibit typical cracks brought by flexural bending loading.

The cracks and failure patterns between the GRC beam and reinforced CRC beams show similarities. Research conducted by both Sumajouw & Rangan [47] and Setiati & Irawan [58] with fewer reinforcement designs shows that the initial cracks formed in the beams occur in the pure bending zone at the mid-span area, precisely at the bottom of the load.

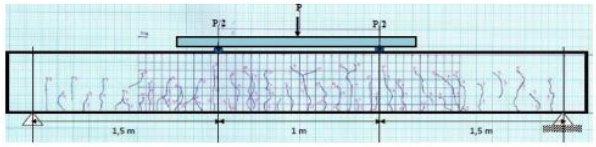

(a)

(b)

Fig.9 Failure pattern of the beams: (a) Conventional Reinforced Concrete Beam [56];

(b) Geopolymer Reinforced Concrete Beam [47].

Similar to other cases, some flexural fractures in the shear span of beams with higher tensile reinforcement ratios became inclined cracks as a result of the shear force. Along the span, the cracks' width and spacing changed. Overall, the crack patterns found in GRC beams were comparable to those found in CRC beams. When the compression face of the concrete beams was ultimately crushed, the longitudinal compressive steel also buckled. The mechanism was typical of an under-reinforced beam failure [47].

Fig. 10 RCC and GPC Beam Crack Pattern [52]

Table 2. Beam Failure modes, Crack Width, and Initial Crack Load.

Authors	Beam ID	Beam Types	Type of Failure
Kumaravel S et. Al [52]	CRC-I	Conventional Reinforced Concrete (CRC) Beams	Flexural mode
	CRC-II		Flexural mode
Sumajouw DMJ, Rangan BV [47]	GRC-I	Geopolymer Reinforced Concrete (GRC) Beams	Flexural mode
	GRC-II		Flexural mode
		Crack Width (mm) at Service Load-40 kN	
Dattatreya JK et.al [54]	CRC-1	0.125	Flexural mode
	CRC-2	0.210	Flexural mode
	CRC-3	0.230	Flexural mode
	FAB1	-	Flexural mode
	FAB2	0.130	Flexural mode
	FAB3	0.280	Flexural mode
	GRC-1	0.180	Flexural mode
	GRC-2	0.240	Flexural mode
	GRC-3	0.450	Flexural mode
		Beam Types	First Crack Load (kN)	
Abraham R et.al [53]	CRC_1	Conventional Reinforced Concrete (CRC) Beams	16.75	Flexural mode
	CRC_2		18.5	Flexural mode
	CRC_3		20	Flexural mode
	CRC_4		24	Flexural mode
	GRC_1	Geopolymer Reinforced Concrete (GRC) Beams	18	Flexural mode
	GRC_2		20	Flexural mode
	GRC_3		22	Flexural mode
	GRC_4		24	Flexural mode

Figures 9 b and 10 illustrate that the cracking patterns and failure mechanisms shown for GRC beams are identical to those observed for CRC beams. This is by studies [47 and 52]. The failure processes of the CRC beams and GPC beams are displayed by the flexure behavior in Table 2 [47] and [52].

The same situation also arises in Dattatreya et al.'s experimental research [54]. In general, the GRC beam specimens developed flexural cracks in identical order to the CRC beam specimens for any given load. The failure modes of the two types of beams were essentially identical, and the crack pattern at various phases was also very similar. As shown in Table 2, flexure modes are the causes of failure for CRC and GRC beams, and both beams have similar fracture widths, crack spacing, and crack numbers.

According to a study by Abraham et al. [53], the observed GRC beam crack patterns were almost identical to those in CRC beams under all conditions. Because the load was increased linearly at first, cracks were originally not seen during the test. Using the load increase, flexure cracks started to appear as predicted in the bending zone at the center of the beams. The span experience both the development of new cracks and the widening of

existing cracks as the load increased. Table 2 [52, 47, 53, 54] displays the crack patterns of both beams.

During the test, Ojha, P.N. et al. [55] noted the crack pattern for both beams. Flexural cracks first became apparent at the very beginning of loading, and spread at the tension zone between the loading arrangements. Figures 11 (a) and (b) demonstrated how normal-strength CRC beams and normal-strength (M40) GRC beams have fewer and smaller visible cracks, respectively. High-strength (M70) CRC beams and the equivalent GRC beams have identical crack patterns and sizes.

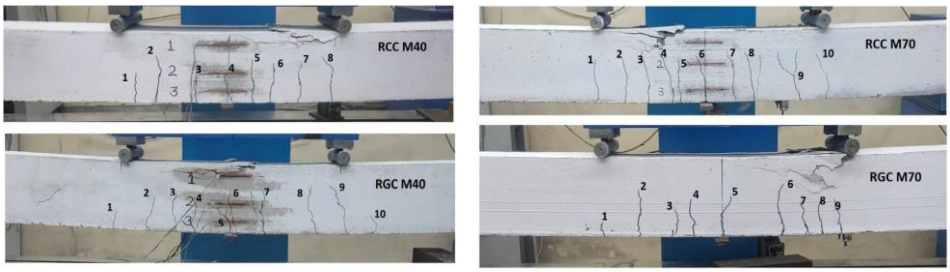

(a) M40 CRC and GRC (b) M70 CRC and GRC

Fig. 11 Cracks width and pattern [55]

For all cases, when the applied load approaches the cracking moment limit, cracks initiate to develop on the tension side of the beams and begin to extend upward. Typically the first cracks appear at the tested GRC and CRC beams at comparable stress values in the middle of the span and spread upwards. More flexural cracks develop at the mid-span and near the support areas as the load increases, and the pre-existing vertical cracks significantly widen and deepen. Vertical cracks near the supports begin to develop inclined cracks when the loading is increased even further. The reinforcing ratio affects the number, and distribution of cracks as well as the size and length of the cracks. As the beam is designed for under-reinforced conditions, the failure modes of all beams occur by yielding steel reinforcement followed by reaching failure strain on the concrete.

4.2. Failure Load Parameters

The designed failures of under-reinforced concrete beams are comparable to the failure load of GRC and CRC beams. Every beam fails in the flexural phase. However, compare to CRC beams, the failure of GRC beams is more ductile, and followed by concrete in the compression zone being crushed. Table 3 displays the failure loads for both beams [53] and [52].

The expected failure loads [52] were calculated by using FEA software (ANSYS). It demonstrated that the failure load of the test results was very close to the calculated results. Table 3 compares the failure loads of CRC beams and GRC beams. As predicted, the tensile steel first yield, then the concrete in the compression face is crushed.

Numerous studies have investigated the failure behavior of CRC beams under flexure. The majority of the examinations were carried out on typical reinforced concrete beams with longitudinal reinforcement, and higher compressive strength. Table 4 displays the load-carrying capacities at different stages [54]. It demonstrates that, despite GRC beams' somewhat higher compressive strength, the load at the beginning of the initial crack is nearly identical in the case of CRC and GRC beams. Due to their slightly lower flexural rigidity than CRC beams, GRC beams also demonstrate reduced service load and ultimate load-carrying capability. The GRC beams have bigger maximum load-carrying capacities

than the CRC beams, and this is due to their greater compressive strength, this might be the case. The beams' final failure involves concrete crushing in the compression zone after the yielding of the tensile steel. This review generally confirms the performance of both beams, and that the load-carrying capability of GRC beams is comparable to that of CRC beams [55].

Table 3. Evaluation of the beam Failure loads [53] and [52]

Authors	Beam types	Beam ID	Failure loads (KN)		
Abraham R et.al [53]	Conventional Reinforced Concrete (CRC) Beams	CRC_1	58.25		
		CRC_2	60.25		
		CRC_3	76.00		
		CRC_4	88.00		
	Geopolymer Reinforced Concrete (GRC) Beams	GRC_1	59.25		
		GRC_2	69.75		
		GRC_3	82.00		
		GRC_4	88.00		
			Failure loads (kN)		
			Test result	Predicted result (ANSYS)	Failure loads (kN)
Kumaravel S et.al [52]	Conventional Reinforcement Concrete (CRC) Beams	CRC_1	72.00	75.00	96.0
		CRC_2	74.50	75.00	99.3
	Geopolymer Reinforced Concrete (GRC) Beams	GRC-I	74.00	77.50	95.5
		GRC-II	76.50	77.50	98.7

4.3. Loads and Deflection Relationship

The load and deflection relationship between GRC beams and CRC beams exhibit an excellent correlation, according to Dattatreya et al. [54]. Figures 12. a and 12. b represent the mid-span deflection for the two specimens. For CRC beams and just a little bit more for GRC beams, the first crack deflection was a lesser amount than 1% of the ultimate deflection. The higher elastic modulus of CRC beams was what gives better serviceability.

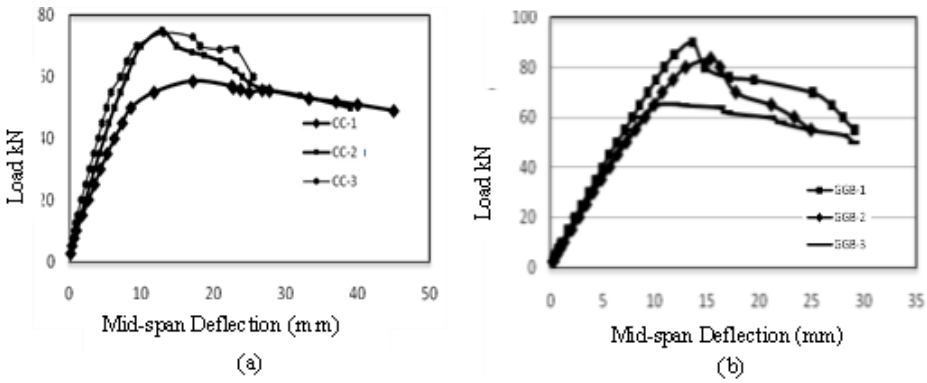

Fig. 12 Deflection at mid-span for both Beams [54]

According to Sumajouw and Rangan [47], in the case of GRC beams, the load and deflection relationship was a sign of the important steps that were performed throughout the test (Figure 13). All the beams perform in a distinctive manner that is consistent with Figure 2 the typical relationship between the load-deflection curve [59].

Table 4. Load-carrying capacities at various stages [54-55]

Authors	Beam ID	Service Load (kN)	First Cracking Load (kN)	Yield Load (kN)	Ultimate Load (kN)
Dattatreya JK et.al [54]	CRC-1	39.0	9.5	58.90	58.90
	CRC-2	48.0	10.0	75.65	75.65
	CRC-3	56.0	10.0	79.65	79.65
	FAB1	26.0	6.75	37.50	37.50
	FAB2	38.0	9.5	84.74	84.74
	FAB3	39.0	8.75	89.80	89.80
	GRC-1	48.0	10.0	90.60	90.60
	GRC-2	45.0	10.0	85.45	85.45
	GRC-3	44.0	8.0	69.75	69.75
Ojha PN et.al [55]		Compressive Strength			P_y/P_u
	CRC Beam-1-M40	46.11	60.25	159.90	98.40
	CRC Beam-2-M40	44.61	64.75	161.90	97.77
	GRC Beam-1-M40	50.72	66.85	171.10	95.75
	GRC Beam-2-M40	51.47	57.90	159.90	96.44
	CRC Beam-1-M70	82.15	79.92	222.70	98.06
	CRC Beam-2-M70	83.90	82.25	224.60	96.56
	GRC Beam-1-M70	77.80	87.65	227.10	99.00
	GRC Beam-2-M70	79.80	80.75	224.00	96.34

By Abraham et al. [53] the ductility factor was calculated by plotting the load versus deflection curve using the measured values. The load-deflection behavior of GRC and CRC beams using various steel reinforcement ratios is depicted in Figure 14. Additionally, it can be seen that both beams' load-deflection behavior is identical in nature.

According to Kumaravel et al. [52], as shown in Figure 15, the mid-span deflection gained for the CRC beams and GRC beams almost have identical curvature. The GRC beams behave similarly to control beams based on the load and mid-span deflection. When compares to CRC beams, GRC beams have a higher ultimate load capacity (Figure 15).

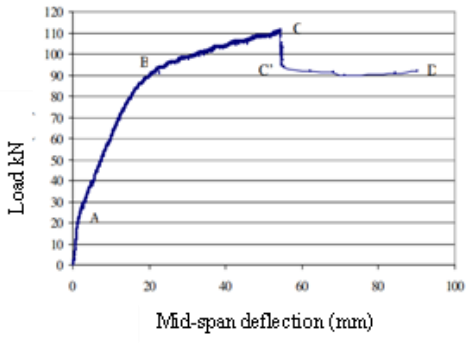

Fig. 13 Deflection at mid-span for GPC Beam [47]

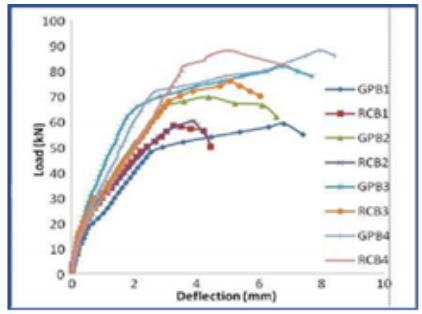

Fig. 14 Deflection at mid-span of the Beam [53]

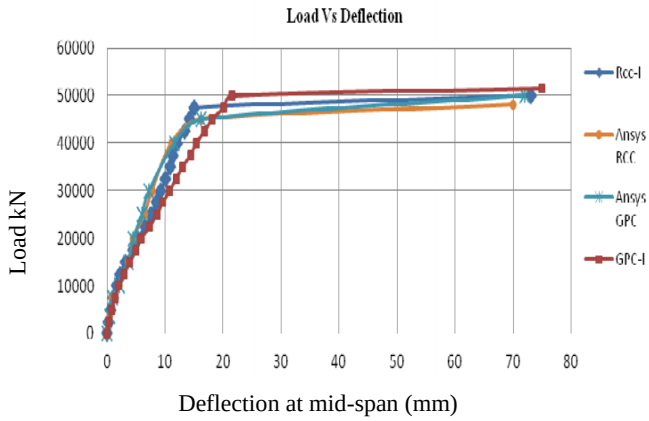

Fig. 15 Mid-span deflection of Beam [52]

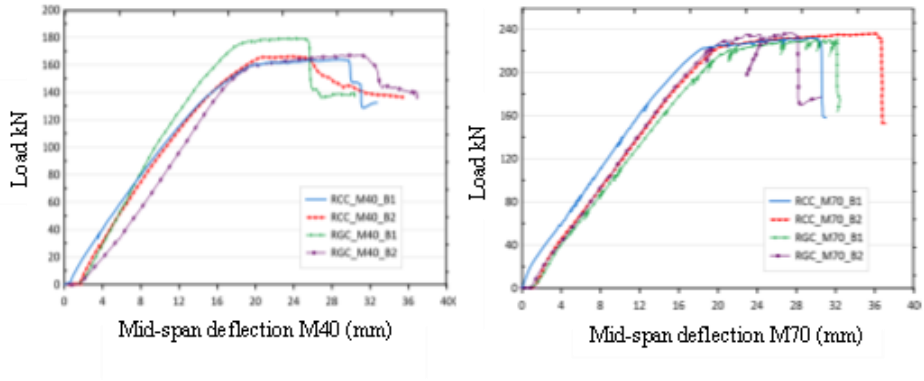

Fig. 16 Mid-span deflection of the Beam [55]

The load versus displacement curves for GRC and CRC beams made of M40 and M70 grade concrete are shown in Figure 16. The load-deflection curve was used to directly identify the yield point. All of the beams' deflection increased linearly up until the first crack was

detected. The failure was indicated by the decrease in curvatures for all combinations. The curves indicate that both kinds of beams exhibit similar flexural behavior. Using IS 456 [55], the expected moment values are determined.

The findings show that the load-deflection curves for all studies of GRC beams are similar to three regions for the typical relationship of load-deflection of CRC beam as shown in Figure 2 [59]. The uncracked state of the beams is represented by the sharp linear response in the first section (region 1). Once the load exceeds the tensile strength of concrete or the modulus of rupture, the constant moment zone of the CRC beams begins to crack. After that point, the curves shift to the second section called a post-crack load level (region II), which represents the beams' cracked state. This segment, which continues until the peak compressive strain, has a lower slope compared to the first segment because of expanding cracking. The load decreases every time a significant crack shows up. Following the second segment, which experiences a beam rupture due to concrete crushing, is the third segment, called post serviceability level (region III). Based on the CRC's mechanical and material characteristics, this segment exhibits a nonlinear response.

4.4. Deflection Parameters

According to [56], based on the calculation from equation (3), the maximum amount of deflection of the GRC beam was larger than the CRC beam. This was due to the specific gravity of the GRC beam being larger but having a smaller modulus of elasticity compared to the CRC beam. This was obvious from the mid-span load deflection that the GRC beams behave similarly to the control beams (Table 5).

As stated by [53], the deflection of all beams developed linearly and remained proportional to load until the appearance of the first cracks. It was discovered that GRC beams exhibit greater deflection at ultimate load than CRC beams. Furthermore, it was found that the load-deflection behavior of CRC and GRC beams was identical. The capacity of energy absorption of the GRC beams had been improved by their greater load-carrying capacity and larger deflections as shown in Table 5 [53].

According to [52], the test and predicted result (ANSYS) of load-deflection curves were comparable for both GRC beams and control beams as shown in Table 5. The investigation by Abraham et. al [53] and Kumaravel et. al. [52] found that the deflection values carried by GRC beams were greater than CRC beams. But overall, the carried-out value of the deflection of the tests is proportional to the calculation results.

Figure 13 displays the mid-span deflection curve created by Sumajouw and Rangan [47], while Table 7 displays the greatest deflection. These characteristics describe reinforced concrete beams' typical flexure behavior [59]. In Figure 2, at points A, B, C, C' dan D, the gradual increment of deflection as an increasing load function is displayed. The deflection curves show specific instances of what happened during the test. The final load and mid-span deflection for CRC beams and GRC beams, which are studied by [47], are shown in Figure 13.

Dattatreya et al [54] claimed that a comparable technique was used to obtain the peak load deflection. When compared to the actual measurements, the testing load and the corresponding predicted deflections revealed a generally acceptable agreement. In general, there was good agreement between the test result of deflections and the calculated deflections that were computed according to the provisions of IS 456:2000, and conventional CRC theory.

The deflection response of CRC elements is a complicated process with a wide variety of impacts, such as differing strength and deformation characteristics of steel and concrete, cracking, and bond slip between reinforcement and concrete. Concrete between cracks

increases stiffness whereas the impact of reinforcing is dominant when the beams are cracked. Generally, it finds in this review, that GRC beams often show greater deflection than CRC beams at service load and peak load levels, as well as other load levels. Furthermore, multiple investigations for fly ash-based low calcium GRC beams show that these beams have an equivalent initial load to crack, crack width, deflection, ultimate load, and failure mechanism to CRC beams undergoing flexural stress. [47, 52, 53, 54].

Table 5. Comparison of Deflection values [56, 53, 52]

Authors	Beam ID	Load at First Cracking (kN)	Crack at Mid-Span Deflection (mm)	Maximum Deflection (mm)
Setiati NR, Irawan RR. [56]	CRC-B1	18.59	2.26	10.553
	CRC-B2	19.41	2.52	
	GRC-B1	20.34	2.32	11.365
	GRC-B2	20.16	2.60	

Authors		Ultimate Load Deflection (mm)	The capacity of Energy absorption (kNmm)
Abraham R, et.al [53]	CRC_1	3.273	122.392
	CRC_2	3.92	161.797
	CRC_3	5.071	269.756
	CRC_4	5.016	284.583
	GRC_1	6.814	320.181
	GRC_2	4.397	216.347
	GRC_3	6.762	433.700
	GRC_4	7.98	531.781

Authors		Deflection (mm)		Ratio between Test/ Predicted result
		Test result	Predicted result (ANSYS)	
Kumaravel S, et.al [52]	CRC-I	73.00	70.00	1.04
	CRC-II	70.00	70.00	1.00
	GRC-I	75.00	72.00	1.04
	GRC-II	76.00	72.00	1.06

4.5. Ductility Index Parameters

Table 6 displays the ductility index, which was determined by the load-displacement and moment-curvature [53]. All GRC beams have better curvature ductility values than the corresponding CRC beams. All specimens failed in a flexural mode, but the failure of GRC beams was more ductile than that of CRC beams and was followed by concrete being crushed in the compression zone, providing additional proof that all of the beams failed in tension.

Table 6. Comparison of Ductility Index [53]

Beam Types	Beam ID	Bending Behavior	
		Displacement Ductility Index	Curvature Ductility Index
Conventional Reinforcement Concrete (CRC) Beams	CRC_1	2.98	7.72
	CRC_2	1.64	3.59
	CRC_3	1.85	3.47
	CRC_4	1.11	1.24
Geopolymer Reinforced Concrete (GRC) Beams	GRC_1	5.12	8.17
	GRC_2	2.68	3.68
	GRC_3	4.30	4.94
	GRC_4	1.44	1.38

The ductility is calculated by dividing the deflection at the ultimate moment by the deflection at the yield moment [47]. The yield moment, My is calculated for this purpose using the elastic theory [59]. The load-deflection test curves shown in Figure 13 are used to calculate the deflections related to the yield moment (My) and ultimate moment (Mu).

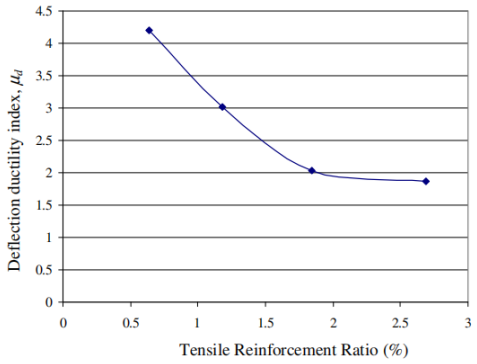

Fig. 17 Ductility Index of Tensile Reinforcement Ratio (GBI Series) [47]

Figure 17 depicts the effect of tension reinforcement on the ductility index. This graph shows how the ductility index declines with increasing tensile reinforcement. Deflection ductility increases significantly in specimens with a reinforcement ratio of less than 2.0%; however, deflection ductility is only marginally affected in beams with a reinforcement ratio of more than 2.0%. These test trends reflect those that are seen with CRC concrete beams [59]. The ductility index of test beams is provided in Table 7 as previously mention.

Study [54] found that the proportion of curvature at peak load to ultimate curvature at failure varied between 1.47 to 1.75 for GRC beams compared with 1.38 to 2.33 for CRC beams, indicating that GRC beams have less post-peak ductility than CRC beams. For GRC specimens, the deflections at several phases, together with the service and peak load phases, were higher. The ductility factor was similar to CRC beams. The review of all types of beams confirms that ultimate moment capacity and deflection for GRC flexural beams could be calculated using the CRC beam theory.

Table 7. Index of Ductility and Mid-span Deflection at Failure Loads [47]

Beam ID	Compressive Strength	Reinforcement Ratio (%)	Deflection (mm)	Ductility Index
GRC-I.1	37.0	0.64	56.53	4.20
GRC-I.2	42.0	1.18	46.01	3.01
GRC-I.3	42.0	1.84	27.87	2.03
GRC-I.4	37.0	2.69	29.22	1.87
GRC-II.1	46.0	0.64	54.27	3.8
GRC-II.2	53.0	1.18	47.20	3.28
GRC-II.3	53.0	1.84	30.01	2.25
GRC-II.4	46.0	2.69	27.47	1.70
GRC-III.1	76.0	0.64	69.75	4.95
GRC-III.2	72.0	1.18	40.69	3.24
GRC-III.3	72.0	1.84	34.02	2.74
GRC-III.4	76.0	2.69	35.85	2.41

4.6 Correlation of Test to Predicted Result

Sumajouw and Rangan [47] determined the GRC flexural strength according to the AS3600 specification for concrete structures [58]. Table 8 and Figure 18 compare the results of the evaluations with the estimated values. The overall ratio of test to expected results was 1.11, with a standard deviation of 0.135. The ultimate moment capacity was computed using IS456 in the study by Dattatreya et al. [54] with standard deviations of 0.142.

The borderline of the ultimate moment between the test results and the theoretical calculation shows the agreement as presented in Table 8 concerning the comparison ratio between the two values. The relationship in the form of a diagram shows in Figure 18.

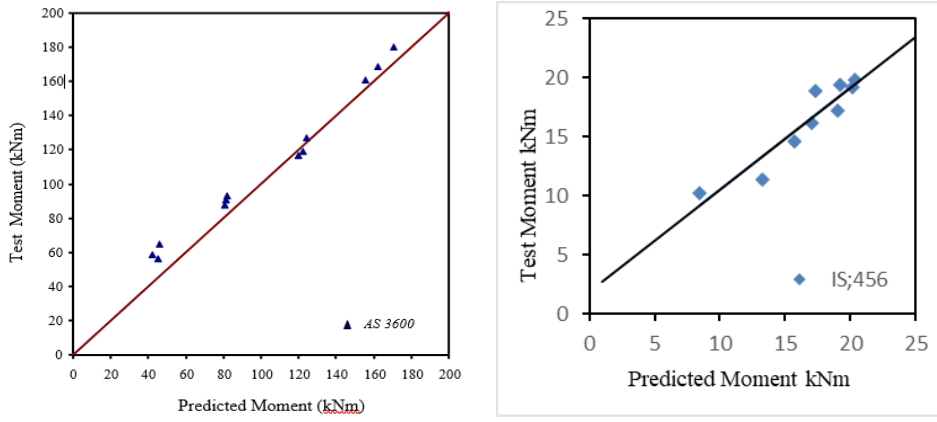

(a) AS 3600 [47] (b) IS 456 [54]

Fig.18 Predicted and test results

The experimental maximum moment (Me) of beams was calculated as per the dimensions of the beam and the reinforcements following IS 456:2000. The moment of resistance (Mp) was calculated as per IS-456. The experimental maximum value was obtained from beam testing of mid-span. Table 9 shows the ratio between the test to predicted results [55].

Table 8. Evaluation of predicted and test results based on AS 3600 [47] and IS 456 [54]

Authors	Beam ID	Ultimate Moment (kN-m)		Ratio between Test / Predicted result
		Test result	Predicted result (AS3600)	
Sumajouw DMJ, Rangan BV. [47]	GRC-I.1	56.30	45.17	1.24
	GRC-I.2	87.65	80.56	1.09
	GRC-I.3	116.85	119.81	0.98
	GRC-I.4	160.50	155.31	1.03
	GRC-II.1	58.35	42.40	1.28
	GRC-II.2	90.55	81.50	1.11
	GRC-II.3	119.00	122.40	0.97
	GRC-II.4	168.70	162.31	1.04
	GRC-III.1	64.90	45.69	1.42
	GRC-III.2	92.90	82.05	1.13
	GRC-III.3	126.80	124.17	1.02
	GRC-III.4	179.95	170.59	1.05
		Average number		1.11
		Standard Deviation		0.135
Dattatreya JK et.al [54]	CRC-1	13.25	11.44	1.24
	CRC-2	17.03	16.19	1.05
	CRC-3	17.33	18.87	0.92
	FAB1	8.44	10.25	0.82
	FAB2	19.06	17.18	1.28
	FAB3	20.21	19.22	1.05
	GRC-1	20.39	19.78	1.03
	GRC-2	19.24	19.41	0.99
	GRC-3	15.71	14.62	1.07
		Average		1.05
		Standard Deviation		0.142

Table 9. The maximum strength of Beams [55]

Beam Code	Compressive Strength (MPa)	Moment (kN-M)		Predicted Moment M_p (kN-M)	Ratio between Test/Predicted result M_e/M_p
		Yield	Ultimate M_e (Experimental)		
M40 CRC Beam - 1	46.11	53.30	54.17	44.01	1.23
M40 CRC Beam - 2	44.61	53.97	55.20	44.01	1.25
M40 GRC Beam - 1	50.72	57.03	59.57	44.01	1.35
M40 GRC Beam - 2	51.47	53.30	55.27	44.01	1.26
M70 CRC Beam - 1	82.15	74.23	75.70	67.37	1.12
M70 CRC Beam - 2	83.90	74.87	77.53	67.37	1.15
M70 GRC Beam - 1	77.80	75.70	76.47	67.37	1.14
M70 GRC Beam - 2	79.80	74.67	77.50	67.37	1.15

5. Conclusions

This paper presents significant findings and results along with the current grouping parameters to analyze the flexural behavior of GRC and CRC beams. After conducting a critical review, the conclusion is as follows:

- The crack patterns and failure mechanisms mentioned in the literature for CRC beams are found to be equivalent to those considered for GRC beams. All beams collapse in flexure in a ductile way as the steel reinforcing yield in tension and the concrete is crushed in the area known as the compression zone.
- The flexural behavior of both GRC and CRC beams in load-deflection relationships exhibits a typical similarity to the description of significant test steps. These stages are listed in the following order; initial crack, yielding of the tensile steel, the concrete crushing associated with spalling of the concrete cover, and disintegration of the concrete compression zone due to buckling of the longitudinal steel at the compression area.
- The comparison between predicted and test results indicates that the deflection performance of GRC and CRC beams is nearly identical. Furthermore, the calculated deflection values based on AS3600 serviceability provisions are compared to the observed deflection during testing, and a good agreement is observed between the two. The test to calculated deflection ratio has a mean value of 1.15 and a standard deviation of 0.06, indicating a reasonably close match between the experimental and computed values. Additionally, there is reasonable agreement between the deflection test results and the predicted deflections calculated using the guidelines of IS456:2000 (Indian Standard Code for Plain and Reinforced Concrete) and CRC theory.
- The ductility of GRC beams increases as the tensile reinforcement ratio decreases, specified by the ratio of mid-span deflection at the ultimate moment to mid span

deflection at the yield moment. According to test results, ductility increases significantly with ratio of beam's tensile reinforcement of smaller than 2%. The ductility is only slightly influenced by tensile reinforcement ratios of higher than 2%. These test patterns match the behavior of CRC beams closely.

- There is a comparable relationship between the test and predicted values for the test beams when the ultimate moment carrying capacities are calculated using the CRC principles and strain compatibility approach. On top of that, according to the findings, GRC beams can be evaluated using the same computational techniques that are used to assess the performance parameters of CRC beams at various phases. It has been confirmed that the design guidelines in the Indian Standard (IS 456) and Australian Standard for Concrete Structures (AS3600) for CRC apply to GRC beams. Therefore, it might be concluded, the behavior of GRC and CRC beams depicts a similar type, thus the standards that are developed for CRC, can also certainly be applied to GRC beams.

References

[1] Blaszczynki TT, Krol MM. The durability of Green-Concrete, Proceedings of 8th International Conference AMCM, Poland. 2014; 530-540.
[2] Davidovits J. Global Warming Impact on the Cement and Aggregates Industries, World Resource Review. 1994; 6(2): 263-278.
[3] Kaya M. Mechanical properties of ceramic powder-based geopolymer mortars. Magazine of Civil Engineering. 2022. 112(4). Article No. 11207.
[4] Sumajouw DMJ, Malingkas G, Pandaleke R, Handono BD. Geopolymer Concrete (GPC) as a Suitable Green Solution for Building and Construction Material, Journal of Mechanical and Civil Engineering (IOSR-JMCE). 2023; 20: 61-72
[5] Davidovits J. Chemistry of Geopolymeric Systems, Terminology. In: Joseph Davidovits, Davidovits R, James C, editors. Geopolymer '99 International Conference; 1999 June 30 to July 2, 1999; France; 1999; 9-40.
[6] Xu H, van Deventer JSJ. Geopolymerisation of Multiple Minerals. Minerals Engineering 2002;15(12):1131-1139. https://doi.org/10.1016/S0892-6875(02)00255-8
[7] Palomo A, Grutzeck MW, Blanco MT. Alkali-Activated Fly Ashes, A Cement for the Future. Cement and Concrete Research 1999; 29(8):1323-1329. https://doi.org/10.1016/S0008-8846(98)00243-9
[8] Xu H, van Deventer JSJ. The Geopolymerisation of Alumino-Silicate Minerals. International Journal of Mineral Processing 2000; 59(3): 247-266. https://doi.org/10.1016/S0301-7516(99)00074-5
[9] van Jaarsveld JGS, van Deventer JSJ, Lukey GC. The Effect of Composition and Temperature on the Properties of Fly Ash and Kaolinite-based Geopolymers. Chemical Engineering Journal 2002; 89(1-3): 63-73. https://doi.org/10.1016/S1385-8947(02)00025-6
[10] Swanepoel JC, Strydom CA. The utilization of fly ash in a geopolymeric material. Applied Geochemistry 2002;17(8):1143-1148. https://doi.org/10.1016/S0883-2927(02)00005-7
[11] Barbosa VFF, MacKenzie KJD, Thaumaturge C. Synthesis and Characterisation of Materials Based on Inorganic Polymers of Alumina and Silica: Sodium Polysialate Polymers. International Journal of Inorganic Materials 2000; 2(4): 309-317. https://doi.org/10.1016/S1466-6049(00)00041-6
[12] Standards-ASTM, Standard Test Method for Length Change of Hydraulic-Cement Mortars Exposed to a Sulfate Solution. 1995; C 1012 -95a.
[13] Hime WG. Comments on Geopolymer Concrete. 2003.

[14] Li G, and Zhao X. Properties of concrete incorporating fly ash and ground granulated blast-furnace slag. Cement & Concrete Composites, 2003; 25(3): p. 293-299. https://doi.org/10.1016/S0958-9465(02)00058-6
[15] Cheng TW, Chiu JP. Fire-resistant Geopolymer Produced by Granulated Blast Furnace Slag. Minerals Engineering. 2003; 16(3): 205-210. https://doi.org/10.1016/S0892-6875(03)00008-6
[16] Hardjito D. Wallah SE, Rangan BV. Study on Engineering Properties of Fly Ash-Based Geopolymer Concrete. Journal of the Australasian Ceramic Society 2002; 38(1): 44-47.
[17] Hardjito D, Wallah SE, Sumajouw DMJ, Rangan BV. Fly Ash-Based Geopolymer Concrete. Australian Structural Engineering Journal, Engineers Australia, 2005. https://doi.org/10.1080/13287982.2005.11464946
[18] Hardjito D, Wallah SE, Sumajouw DMJ, Rangan BV. On The Development of Fly Ash-Based Geopolymer Concrete. ACI Materials Journal, American Concrete Institute, December 2004. https://doi.org/10.1080/13287982.2005.11464946
[19] Hardjito D, Wallah SE, Sumajouw DMJ, Rangan BV. Introducing Fly Ash-based Geopolymer Concrete: Manufacture and Engineering Properties. In Proceedings of the International Conference Our World in Concrete, Singapore, August 2005. https://doi.org/10.1080/13287982.2005.11464946
[20] Sumajouw DMJ, Hardjito D, Wallah SE, Rangan BV. The Behavior of Geopolymer Concrete Columns Under Equal Load Eccentricities. In: Proceedings of the Seventh International Symposium on Utilisation of High Strength/High-Performance Concrete; Washington DC, USA: American Concrete Institute; June 2005.
[21] Sumajouw DMJ, Hadrjito D, Wallah SE, Rangan BV. Flexural Behaviour of Reinforced Fly Ash-Based Geopolymer Concrete Beams. In Proceedings of CONCRETE 05 Conference, Melbourne, Concrete Institute of Australia, October 2005. https://doi.org/10.1080/13287982.2005.11464946
[22] Wallah SE, Hardjito D, Sumajouw DMJ, Rangan BV. Creep and Drying Shrinkage Behaviour of Fly Ash-Based Geopolymer Concrete. In Proceedings of CONCRETE 05 Conference, Melbourne, Concrete Institute of Australia, October 2005. https://doi.org/10.1080/13287982.2005.11464946
[23] Wallah SE, Hardjito D, Sumajouw DMJ, Rangan BV. Sulfate and Acid Resistance of Fly Ash-Based Geopolymer Concrete. In Proceedings of the Australian Structural Engineering Conference, Newcastle, Engineers Australia, September 2005. https://doi.org/10.1080/13287982.2005.11464946
[24] Davidovits J. Geopolymers: Inorganic Polymeric New Materials. Journal of Thermal Analysis, 1991; 37: 1633-1656. https://doi.org/10.1007/BF01912193
[25] Davidovits J. Properties of Geopolymer Cements. In: First International Conference on Alkaline Cements and Concretes; 1994; Kyiv, Ukraine, 1994: SRIBM, Kyiv State Technical University, 1994; 131-149.
[26] Davidovits J. High-Alkali Cements for 21st Century Concretes. Concrete Technology, Past, Present, and Future, In proceedings of V. Mohan Malhotra Symposium. Editor: P. Kumar Metha, ACI SP- 144, 1994; 383-397.
[27] Nath P, Sarker PK. Use of OPC to improve the setting and early strength properties of low calcium fly ash geopolymer concrete cured at room temperature, Cement & Concrete Composites Journal, 2014; (55): 205-214. https://doi.org/10.1016/j.cemconcomp.2014.08.008
[28] Krishnaraja AR, Sathishkumar NP, Kumar TS, Kumar PD. Mechanical Behavior of Geopolymer Concrete under Ambient Curing, International Journal of Scientific Engineering and Technology, 2014; 3(2): 130-132.
[29] Nath P, Sarker PK, Rangan BV. Early age properties of low-calcium fly ash geopolymer concrete suitable for ambient curing, The 5th International Conference of Euro Asia Civil Engineering Forum (EACEF-5), 2015. https://doi.org/10.1016/j.proeng.2015.11.077

[30] Shinde BH, and Kadam KN. Properties of Fly Ash based Geopolymer Mortar with Ambient Curing, International Journal of Engineering Research, 2016; (5): 203-206.
[31] Manjunath G, Giridhar C. Compressive strength development in Ambient Cured geopolymer mortar, International Journal of Earth Sciences and Engineering, 2011; (4-6): 830-834.
[32] Hardjito D, Rangan BV. Development and Properties of Low-Calcium Fly Ash-based Geopolymer Concrete, Research Report GC-1, Faculty of Engineering, Curtin University of Technology, Perth, 2005.
[33] Kong DL, Sanjayan JG. Damage behavior of geopolymer composite exposed to elevated temperatures, Cement and Concrete Composites, 2008; 30(10): 986-991. https://doi.org/10.1016/j.cemconcomp.2008.08.001
[34] Guo X, Shi H, Dick WA. Compressive strength and microstructural characteristics of Class C fly ash geopolymer, Cement and Concrete Composite, 2010; 32(2): 142-147. https://doi.org/10.1016/j.cemconcomp.2009.11.003
[35] Nasvi M, Gamage RP, Sanjayan JG. Geopolymer as well cement and the variation of its mechanical behavior with curing temperature, Greenhouse Gases: Science and Technology, 2012; 2(1): 46-58 https://doi.org/10.1002/ghg.39
[36] Yost JR, Radlinska A, Ernst S, Salera M, and Martignetti. Structural behavior of alkali-activated fly ash concrete. Part 2: structural testing and experimental findings, Material and Structures Journal, 2013; (46): 449-462. https://doi.org/10.1617/s11527-012-9985-0
[37] Kumar S, Kumar P, Mehrotra S. Influence of granulated blast furnace slag on the reaction, structure, and properties of fly ash geopolymer, Journal of Material and Sciences, 2010; 45(3): 607-615. https://doi.org/10.1007/s10853-009-3934-5
[38] Kumar S, and Kumar R. Mechanical activation of fly ash: Effect on reaction, structure, and properties of resulting geopolymer, Ceramic International, 2011; 37(2): 533-541 https://doi.org/10.1016/j.ceramint.2010.09.038
[39] Sarker PK. Bond Strength of geopolymer and cement concrete, Advances in Science and Technology, 2010; 69:143-151. https://doi.org/10.4028/www.scientific.net/AST.69.143
[40] Sarker PK. Bond strength of reinforcing steel embedded in fly ash-based geopolymer concrete, Mater. Structures, 2011; 44: 1021-1030 https://doi.org/10.1617/s11527-010-9683-8
[41] Sofi M, van Deventer JSJ, Mendis PA, Lukey GC. Bond performance of reinforcing bars in organic polymer concrete (IPC), Journal of Material Sciences, 2007; 42: 3107-3116. https://doi.org/10.1007/s10853-006-0534-5
[42] Hardjito D, Wallah SE, Sumajouw DMJ, Rangan BV. Properties of Geopolymer Concrete with Fly Ash as Source Material: Effect of Mixture Composition. Presented at the Seventh CANMET/ACI International Conference on Recent Advances in Concrete Technology, Las Vegas, USA, 2004.
[43] Hardjito D, Wallah SE, Sumajouw DMJ, Rangan BV. Properties of Geopolymer Concrete With Fly Ash as Its Source Material. Presented at the 21st Biennial Conference Of The Concrete Institute of Australia, Brisbane, Australia: Concrete Institute of Australia, 2003
[44] Wallah SE, Hardjito D, Sumajouw DMJ, Rangan BV. Creep Behavior of Fly Ash-Based Geopolymer Concrete. Presented at the Seventh CANMET/ACI International Conference on Recent Advances in Concrete Technology, Las Vegas, USA, 2004.
[45] Palomo A, Grutzeck MW, Blanco MT. Alkali-activated fly ashes A cement for the future. Cement And Concrete Research, 1999; 29(8): 1323-1329. https://doi.org/10.1016/S0008-8846(98)00243-9
[46] Sumajouw DMJ, Dapas SO. Elemen Struktur Beton Bertulang Geopolymer (Structural Elements for Geopolymer Concretes), Publisher CV. Patra Media Grafindo, Bandung-Indonesia, Third edition, ISBN:978-623-5776-51-4, 2023

[47] Sumajouw DMJ, Rangan BV. Low-Calcium Fly Ash-Based Geopolymer Concrete: Reinforced Beams and Columns, Ph.D. Thesis, Faculty of Engineering, Curtin University of Technology, Perth-Australia, 2006.
[48] Sumajouw DMJ, Hardjito D, Wallah SE, Rangan BV. Fly Ash-Based Geopolymer Concrete: An Application for Structural Members, In Proceeding of the World Congress GEOPOLYMER 2005: Geopolymer; Green Chemistry and Sustainable Development solutions, Saint-Quentin, France, 2005. https://doi.org/10.1080/13287982.2005.11464946
[49] Sumajouw DMJ, Hardjito D, Wallah SE, Rangan BV. Behavior and Strength of Geopolymer Concrete Column, In Proceeding of the 18th Australasian Conference on the Mechanics of Structures & Materials (ACMSM), Perth, A.A. Balkema Publishers, The Netherlands, Perth, Australia, 2004.
[50] Sumajouw DMJ, Hardjito D, Wallah SE, Rangan BV. The behavior of geopolymer Concrete Columns under Equal Load Eccentricities, ACI Special Publication 228, 2005; 577-594.
[51] Sumajouw DMJ, Hardjito D, Wallah SE, Rangan BV. Fly Ash-based Geopolymer Concrete: Studied of Slender Reinforced Columns. Journal of Material Sciences, 2007; 42(9): 3124-3130. https://doi.org/10.1007/s10853-006-0523-8
[52] Kumaravel S, Thirugnanasambandam S, Jeyasehar CA. Flexural Behavior of Low Calcium Fly Ash Based Geopolymer Concrete Beams. International Journal of Engineering and Applied Sciences, 2013; 5(1): 24-31.
[53] Abraham R, Raj DS, Abraham V. Strength and Behavior of Geopolymer Concrete Beams. International Journal of Innovative Research in Science, Engineering and Technology, 2013; 2: 159-166.
[54] Dattatreya JK, Rajamane NP, Sabitha D, Nataraja MC. Flexural Behavior of Reinforced Geopolymer Concrete Beams. International Journal of Civil and Structural Engineering, 2011; 2(1): 138-159.
[55] Ojha PN, Singh B, Trivedi A, Singh P, Singh A, Pede C. Short-term Mechanical Performance and Flexural Behavior of Reinforced Slag-fly Ash-based Geopolymer Concrete beams in Comparison to OPC-based Concrete Beams, Journal of Research Engineering Structures & Materials, 2023; 9(1): 31-51. https://doi.org/10.17515/resm2022.515me0902
[56] Setiati NR, Irawan RR. Perbandingan Sifat dan Karakteristik Beton Geopolymer terhadap Beton Semen Portland untuk Kekuatan Struktur Balok. Jurnal Jalan-Jembatan, 2018; 35(2): 125-138.
[57] Laskar SM, Mozumder RA, Roy B. Behavior of geopolymer concrete under static and Cyclic Loads, Advances in Structural Engineering, 2015; 1643-1653. https://doi.org/10.1007/978-81-322-2187-6_125
[58] Nawy EG. Reinforced Concrete: A Fundamental Approach, Six Edition Prentice Hall-Upper Saddle River, New Jersey, 2009:07458, ISBN-13:978-0-13-241703-7.
[59] Warner RF, Rangan BV, Hall AS, & Faulkes KA. Concrete Structures, Melbourne, Longman, 1999:34010099, ISBN:0 582 802347 4.